Geochemical and isotopic characterization of volcanic and geothermal fluids discharged from the Ecuadorian volcanic arc

S. INGUAGGIATO[1], S. HIDALGO[2], B. BEATE[3] AND J. BOURQUIN[2]

[1]*Istituto Nazionale di Geofisica e Vulcanologia – Sezione di Palermo, Via Ugo La Malfa, Palermo Italy;* [2]*Instituto Geofísico – Escuela Politécnica Nacional, Apartado, Quito, Ecuador;* [3]*Facultad de Geología – Escuela Politécnica Nacional, Quito, Ecuador*

ABSTRACT

The Ecuadorian Quaternary volcanic arc is characterized by about 60 volcanoes many of which are active or potentially active. This volcanic activity is the result of the subduction processes of the Nazca Plate beneath the north-western part of South America. The geochemical signature of the discharged fluids from these volcanic systems gives an important contribution to the comprehension of the subduction processes in the South-American region. In this work, we present the first systematic geochemical characterization of discharged fluids from the entire Ecuadorian volcanic arc on the basis of the chemical and isotopic composition of 56 samples of thermal and cold waters, as well as 32 dissolved and 27 bubbling gases collected from north to south across the arc. The isotopic composition of waters reveals a mainly meteoric origin, while the chemistry of the dissolved gases is characterized by He and CO_2 contents, 2–3 orders of magnitude higher than the air saturated water values, which implies very active gas–water interaction processes with deep fluids. Moreover, both dissolved and bubbling gases' isotopic signature shows a wide compositional range, with helium ranging between 0.1 and 7.12 R/R_a and carbon ranging from −1.75 to −10.50‰ $\delta^{13}C_{(TDIC)}$. Such isotopic features may be related to the presence of at least two distinct end-member sources: the mantle and the crust. Finally, this geochemical study clearly reveals the two distinct geographic parts of the arc, showing different isotopic characteristics of fluids for the Quaternary active volcanism, (north of 2°S), and for the inactive arc, (south of 2°S).

Key words: carbon isotope, ecuador volcanoes, helium isotope, nitrogen isotope, thermal waters

Received 12 April 2010; accepted 7 September 2010

Corresponding author: Salvatore Inguaggiato, Istituto Nazionale di Geofisica e Vulcanologia – Sezione di Palermo, Via Ugo La Malfa, 153 – 90146 Palermo, Italy.
Email: s.inguaggiato@pa.ingv.it. Tel: +39 091 680 9435. Fax: +39 091 680 9449.

Geofluids (2010)

INTRODUCTION

The Ecuadorian Quaternary volcanic arc is characterized by at least 60 volcanoes (Hall & Beate 1991). At least 10 of these volcanoes experienced Holocene eruptions, indicating that they are potentially active; four of them, i.e. Pichincha, Tungurahua, Sangay and Reventador, are currently erupting or have erupted during the last 15 years. Interestingly, most of these Quaternary volcanic edifices display associated hydrothermal systems; fluids related to these hydrothermal sources are the only surface manifestation that can be easily accessed to provide information about the volcanic activity.

Moreover, the collection of fumarolic gases in the summit is difficult and potentially unsafe considering the dimensions of the volcanic edifices, their high altitudes (>4500 masl) and their potential explosive activity.

On the other hand, the Ecuadorian volcanic arc represents a great potential for harnessing geothermal energy in this country, although appraisal of all geothermal prospects is still at an early stage.

In this framework, several geothermal areas along the Ecuadorian Andes have been investigated to provide a preliminary geochemical characterization of the fluids, to discriminate the hydrothermal reservoirs and to identify the
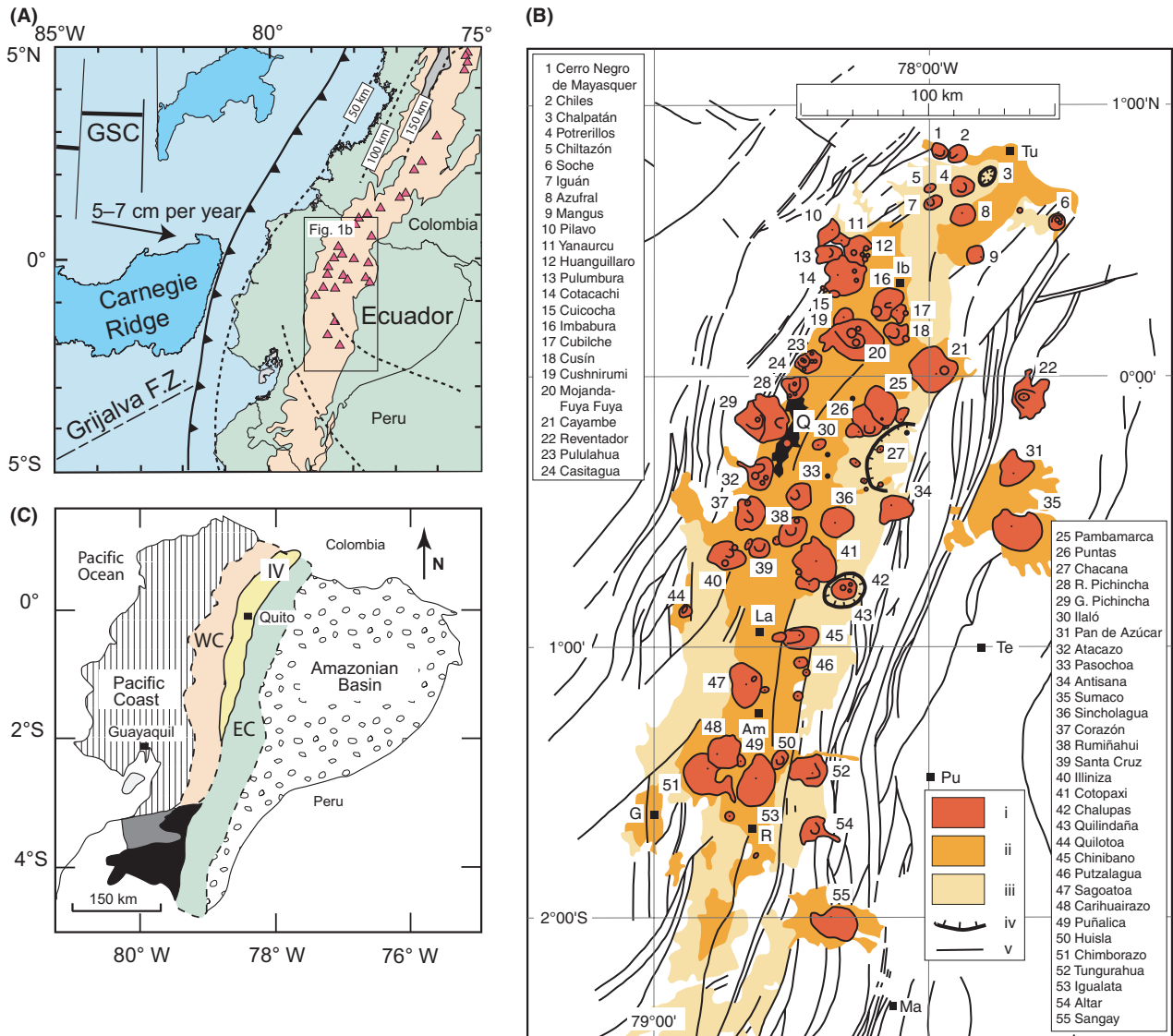
Fig. 1. (A) Geodynamical setting of the Ecuadorian Arc (modified from Gutscher *et al.*, 1999). (B) Ecuadorian volcanoes distribution map from (Hall & Beate 1991). Numbers indicate the different volcanic edifices; i = Quaternary volcanoes, ii = proximal deposits, iii = distal deposits, iv = caldera rim, v = tectonic alignments. (C) Schematic map of the geomorphological/geological zones of Ecuador (modified from Aspden *et al.* 1992a,b). WC = Western Cordillera, EC = Eastern Cordillera and IV = Interandean Valley.

isotopic signature of volcanic and geothermal fluids (mainly He, C, N).

GEODYNAMIC CONTEXT

In Ecuador, magmatism results from the subduction of the Nazca Plate (>22 My in age; Lonsdale 1978; Lonsdale & Klitgord 1978) beneath the North Andean Block, an independent block located in the north-western part of South America (Pennington 1981; Kellogg & Vega 1995; Witt *et al.* 2006). The average rate of convergence is around 58 mm year^{-1} with an almost E–W direction (Trenkamp *et al.* 2002). An interesting geomorphological

feature of this subduction system is the presence of the Carnegie Ridge, which is the product of the uninterrupted interaction of the Galápagos hot spot and the Cocos-Nazca Spreading Centre (Sallarès and Charvis, 2003) (Fig. 1A).

The subducting Carnegie Ridge is covered by a 400–500 m thick sedimentary blanket consisting of carbonate sediments (Michaud *et al.* 2005). Sediments facing the northern Ecuadorian coast line are composed by siliceous nanofossil ooze, chalk and limestone (Hein & Yeh 1983).

The Ecuadorian Quaternary volcanic arc is limited to the south at 2°S and comprises at least 60 volcanic edifices that are distributed in three different domains following a

roughly NNE trench orientation: (i) The Volcanic Front, where the volcanoes are built over the Western Cordillera formations, (ii) the Main Arc, which includes the Interandean Valley volcanoes and the Eastern Cordillera volcanoes and (iii) the Back Arc volcanoes emplaced in the headwaters of the Amazonian basin (Fig. 1B).

The nature and age of the basement of these three volcanic domains are very different, changing from oceanic basalts, dioritic intrusions and volcano-clastic deposits below the Volcanic Front (Goosens & Rose 1973; Lebrat *et al.* 1987; Cosma *et al.* 1998; Reynaud *et al.* 1999; Lapierre *et al.* 2000; Hughes & Pilatasig 2002; Luzieux *et al.* 2006) to older and geochemically more mature continental formations consisting of metasedimentary, igneous and metamorphic rocks under the Main Arc (Aspden & Litherland 1992; Aspden *et al.* 1992b; Litherland *et al.* 1994) (Fig. 1C). South of 2°S, there is no active volcanism, but there are impressive remnants of the Miocene volcanic activity, which are mainly characterized by andesitic to rhyolitic products cropping out as ignimbrites, lava flows and lava domes (Lavenu *et al.* 1992; Beate *et al.* 2001). This old and highly eroded volcanic arc, known as the Saraguro arc, is the host to several porphyry and epithermal ore deposits.

SAMPLING AND ANALYTICAL METHODOLOGIES

On the basis of previous knowledge (Beate & Salgado 2005), several thermal springs, cold water sources and surface waters (rivers) were sampled during a field campaign carried out in January–March 2009. During this field campaign, 49 sampling sites were visited from Tufiño, in northern Ecuador at the border with Colombia, to Portovelo in central-southern Ecuador. Samples 50–57 were collected in August 2009 and include Aguas Calientes (northern Ecuador) and the El Mozo and Puyango sites in the south of the country (Fig. 2). Details on the sites and the related features are given in Table 1.

At every site, the outlet temperature, the electrical conductivity and the pH of the waters were measured using an ORION 250A+ conductivity metre and thermometer and an ORION 250A+ pH-meter, respectively.

Water was sampled in different polyethylene bottles to analyse its major components, silica and ammonium, and its stable isotopes compositions. The samples for cations were acidified with suprapur HNO_3, whereas silica and ammonium analysis were carried out on samples acidified with suprapur HCl. Alkalinity was analysed *in situ* by titration with HCl 0.1 N, whereas major and minor elements were determined in the laboratory using a Dionex 2000i ion chromatograph with an accuracy of ±2%. A Dionex CS-12 column was used for the cations (Li, Na, K, Mg and Ca) and a Dionex AS4A-SC column for the anions (F, Cl, Br, NO_3 and SO_4).

Bubbling gases were sampled using stopcock bottles and Giggenbach bottles (filled with NaOH 4 M and pre-evacuated in laboratory). Gas samples were analysed for the chemical and isotopic composition (He, C and N).

Dissolved gases were sampled and analysed according to the method described by Capasso & Inguaggiato (1998), which is based on the equilibrium partition of gas species between a liquid and a gas phase after the introduction of a host gas (Ar) into the sample. Dissolved gases were analysed using a Perkin Elmer 8500 gas-chromatograph equipped with a 4-m-long Carbosieve S II column and Ar as the carrier gas. He, H_2, O_2, N_2 and CO_2 were measured by means of a TCD detector, while CH_4 and CO were determined through a FID detector coupled with a methanizer. Analyses of the dissolved He isotopic composition were performed using the methodology proposed by Inguaggiato & Rizzo (2004).

The determination of the helium isotopic composition was carried out on a static vacuum mass spectrometer (GVI-Helix SFT) built for the simultaneous detection of ^{3}He and ^{4}He ion beam, to reduce the analytical error down to very low values (an average of ±0.05 R_a). The ^{3}He/^{4}He ratios have been corrected for the atmospheric contamination on the basis of their ^{4}He/^{20}Ne ratios (Sano & Wakita 1985). Values are reported as R/R_a values (where R_a is equal to 1.39×10^{-6}). The δ^{13}C of total dissolved inorganic carbon (TDIC) and the δ^{18}O of H_2O of spring waters were analysed by a Finnigan Delta Plus mass spectrometer. Carbon isotopic values are expressed in δ versus PDB, with an accuracy of 0.2‰. Oxygen isotopic values are expressed in δ versus V-SMOW with an accuracy of 0.2‰.

RESULTS

Surface, cold and thermal waters

Physical parameters

The physical parameters of water samples show a wide range of values. The outlet temperature varied between 7.5 and 74.5°C with the pH ranging between 4.60 and 9.18 and the electrical conductivity from 50 to 68 200 micro-Siemens per cm (Table 1).

These values suggest the occurrence of water/rock and gas/water interaction processes at different degrees. Relatively lower pH (<6) values indicate a possible interaction with acid gases, and high salinity might indicate prolonged water–rock interaction and, in a few cases, evaporation processes.

The relationship between the total dissolved salinity (TDS) and the temperature of waters is shown in Fig. 3. Water samples can be divided into two different groups. The first, consisting in low (<200 mg l^{-1}) salinity waters (river samples) having low temperatures (around 10°C), is dominated by a meteoric contribution. The second group is character-
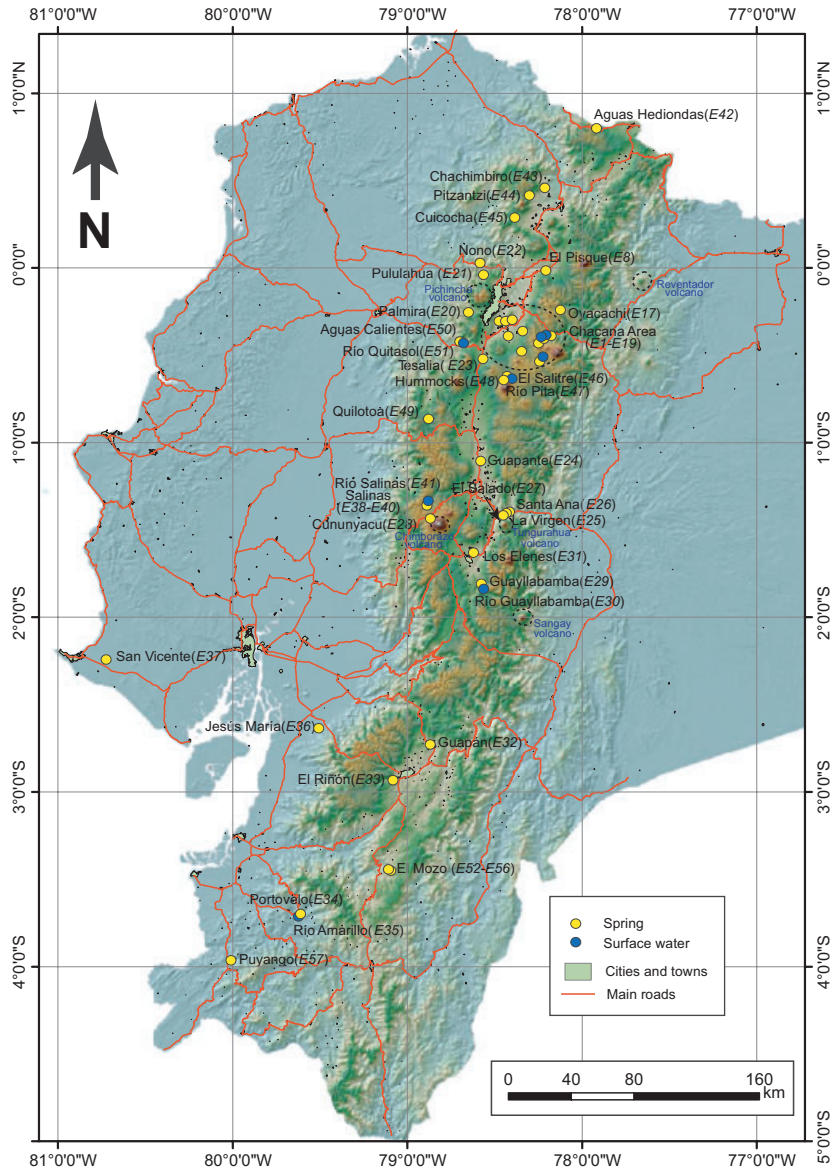
Fig. 2. Location Map of sampled springs.

ized by relatively high outlet temperature (up to 74.5°C) and TDS values up to 10 000 mg l^{-1}, except for few samples like Salinas (54 633 mg l^{-1}), San Vicente (14 229 mg l^{-1}), Guapán (11 353 mg l^{-1}) and Quilotoa (10 931 mg l^{-1}), which seem to have suffered evaporation processes (not shown in Fig. 3). The wide ranges of salinity and temperature, shown by the water samples, suggest different durations and degrees of mineral-dissolution in the waters.

Chemical data

Stable isotopes
δD and δ^{18}O ranges from −104 to −13 ‰ and −13.65 to 4.69 ‰ versus V-SMOW, respectively. Local meteoric

water-line has been reported with the data on Fig. 4A. For a few samples from the Chacana-Papallacta area, a very moderate isotopic shift of oxygen can be observed, suggesting the occurrence of enhanced water–rock interactions. SanVicente, Salinas and Guapán are likely affected by evaporation processes. Interestingly, thermal sources associated with the Quaternary volcanism and those related to the inactive part of the arc plot in two different groups, with the former displaying lower δ^{18}O and δD values. In Fig. 4B, the elevation of each sampling site versus δD values, as well as the theoretical line of vertical isotope gradient for Ecuador (computed on the basis of world water isotope network rain-gauge) is reported. Only about 50% of samples springs fall on the theoretical line show a

Table 1 Chemical and isotopic composition of cold and thermal waters. The chemical composition is expressed in meq l⁻¹. The isotope compositions of δD and δ¹⁸O are expressed in ‰ V-SMOW standard. The carbon isotope composition is expressed in ‰ PDB standard.

Name	Sample	Date	T(°C)	pH	Cond. (uS cm⁻¹)	Eh (mV)	Elevation (masl)	Longitude	Latitude	Li	Na	K	Mg	Ca	F	Cl	Br	SO₄	HCO₃	δ¹⁸O	δD	δ¹³C_TDIC	δ¹³C_CO₂ computed
Cabaña norte	E1	15/1/09	58.9	6.82	3980	103.9	3334	−78 15328	−0 36659	0.35	23.49	0.26	0.30	15.59	0.094	27.46	0.04	11.05	1.30	−11.8	−82	−25.5	−29.2
Fuente del Balneario	E2	15/1/09	47.2	6.56	2900	165.9	3304	−78 15345	−0 36537	0.20	13.33	0.15	0.18	10.06	0.077	13.89	0.29	7.92	1.80	−11.8	−81	−27.1	−31.3
SPA Baja	E3	15/1/09	54.2	7.08	2170	102.4	3278	−78 15171	0 36495	0.20	12.28	0.16	0.14	8.31	0.100	11.32	0.03	7.75	1.65	−11.8	−80	−28.1	−32.8
Jamanco	E4	15/1/09	60.8	6.23	6820	−39	3518	−78 18569	−0 37813	0.95	49.43	1.09	0.67	14.68	0.160	52.80	0.08	6.27	7.45	−11.4	−83	−7.9	−10.1
Río Papallacta	E5	16/1/09	9.0	7.95	105	191	3455	−78 15338	−0 35602	0.00	0.11	0.02	0.20	0.83	0.003	0.40	0.00	0.06	1.03	−11.7	−79	−22.4	−31.7
Río Papallacta	E6	16/1/09	10.5	7.92	181.8	−43	3311	−78 15211	−0 36827	0.00	0.52	0.03	0.20	1.12	0.005	0.40	0.00	0.27	1.20	−11.7	−79		
Fuente El Tambo	E7	16/1/09	57.8	6.15	7250	−40	3550	−78 18707	−0 37935	1.15	56.79	1.53	0.92	13.88	0.180	59.64	0.10	4.93	9.45	−11.5	−82	−7.3	−9.4
El Pisque Balneario	E8	16/1/09	37.0	6.33	2100	21	2633	−78 18071	0 00363	0.00	14.94	1.07	6.80	1.84	0.031	4.90	0.01	0.47	18.95	−13.4	−95	−7.0	−10.7
La Calera de Tolontag	E9	18/1/09	27.2	7.17	5720	81.3	3426	−78 31743	−0 34823	0.28	48.87	1.37	4.35	12.20	0.200	13.91	0.09	27.24	25.85	−11.1	−91	−1.7	−8.3
Balneario La Merced	E10	19/1/09	32.5	6.67	1085	45	2586	−78 39703	−0 29532	0.00	5.18	0.36	4.47	1.98	0.026	1.70	0.01	0.45	9.80	−11.8	−82	−10.2	−14.9
Balneario Ilalo	E11	19/1/09	37.7	6.48	1540	−49.6	2571	−78 38464	−0 29141	0.00	9.13	0.67	6.69	2.90	0.031	3.04	0.01	1.54	14.80	−11.9	−83	−7.8	−11.9
Balneario El Tingo	E12	19/1/09	42.1	7.00	3160	−61	2454	−78 44139	−0 29009	0.00	22.36	0.70	13.93	1.37	0.045	8.33	0.03	1.11	28.80	−13.0	−93	−9.9	−15.2
Cachiyacu campamento	E13	21/1/09	60.1	6.53	5000	−83.7	3918	−78 22868	−0 41175	1.04	35.88	1.88	2.09	4.97	0.050	35.18	0.03	2.44	8.50	−11.4	−85	−5.8	−8.3
Cachiyacu cueva	E14	21/1/09	40.5	5.99	3340	36.5	3926	−78 22948	−0 41388	0.70	24.06	1.30	1.60	5.98	0.050	22.60	0.04	1.81	9.00	−11.6	−85	−4.2	−6.5
Cachiyacu terraza de travertino agua	E16	21/1/09	64.6	6.39	5560	−125	3910	−78 22837	−0 41158	1.16	39.83	2.04	2.72	5.31	0.050	38.15	0.06	2.41	11.02	−11.1	−86		
Balneario Oyacachi	E17	22/1/09	46.5	6.53	4850	−105	3180	−78 09061	−0 21913	0.37	42.56	0.85	4.53	4.94	0.040	18.43	0.01	1.77	33.00	−10.8	−85		
Hacienda Antisana	E18	24/1/09	7.5	6.36	145	284	4045	−78 21844	−0 51552	0.01	0.45	0.09	0.50	0.50	0.060	0.06	0.02	0.21	1.20	−14.6	−110		
Vertiente Río Lisco	E19	24/1/09	29.9	6.10	1780	52.8	3458	−78 31535	−0 46419	0.03	10.35	0.68	5.65	3.00	0.040	6.61	0.02	0.46	12.50	−13.1	−96	−7.8	−10.5
Palmira	E20	13/2/09	25.2	6.79	3300	−4.4	2732	−78 62906	9974200	0.123	23.56	1.21	4.53	10.70	0.040	11.46	0.000	0.01	27.80	−9.4	−73	−7.7	−13.3
Pululahua	E21	14/2/09	25.4		3480	−66.9	2610	−78 54204	0 00573	0.016	17.11	0.16	11.78	16.28	0.000	10.19	0.009	0.00	33.70	−9.4	−65	0.7	−2.4
Nono	E22	14/2/09	27.9	6.28	4050	−88	2578	−78 55913	0 03046	0.225	22.29	0.63	10.91	16.76	0.000	17.70	0.016	0.22	30.60	−9.6	−67	1.7	−2.0
Tesalia	E23	16/2/09	16.8	6.18	1700	174.5	2848	−78 54051	−0 50025	0.016	5.06	0.20	13.25	3.02	0.018	2.32	0.000	0.55	19.00	−12.0	−82	1.5	−2.2
Guapante	E24	17/2/09	24.3	7.13	950	208.6	2531	−78 56898	−1 09662	0.023	4.16	0.34	4.94	1.52	0.019	0.67	0.000	1.84	8.80	−12.9	−92	−4.2	
La Virgen	E25	17/2/09	52.7	6.43	4780	−112.3	1820	−78 41749	−1 39896	0.081	21.77	1.99	33.23	10.24	0.036	11.01	0.000	31.88	26.20	−11.6	−81		
Santa Ana	E26	17/2/09	42.1	6.65	4430	66	1751	−78 40779	−1 39692	0.073	19.97	1.77	31.04	10.72	0.028	9.89	0.000	27.90	26.20	−11.6	−79	−3.0	−7.3
El Salado	E27	18/2/09	45.6	6.40	6770	−51.4	1927	−78 43304	−1 40618	0.093	24.19	2.12	66.98	19.60	0.000	22.59	0.000	63.24	25.60	−11.7	−80	−3.0	−6.4
Cununyacu	E28	18/2/09	47.0	8.37	4300	−88	3670	−78 86584	−1 33816	0.032	27.87	0.20	0.08	14.94	0.000	36.37	0.069	5.53	1.00	−13.7	−104	−2.7	−8.3
Guayllabamba	E29	19/2/09	37.6	6.34	1386	121.8	3238	−78 54624	−1 79124	0.040	8.57	0.36	2.29	5.15	0.029	1.05	0.001	0.01	15.60	−11.9	−83	−6.9	−10.2
Río Guayllabamba	E30	19/2/09	8.6	5.69	83		3238	−78 54624	−1 79124	0.000	0.24	0.06	0.31	0.34	0.003	0.01	0.000	0.02	1.10	−12.3	−84	−6.3	3238
Los Elenes	E31	19/2/09	20.1	7.50	1804	97.5	2590	−78 61006	−1 61885	0.010	8.09	0.27	9.93	4.24	0.090	0.70	0.000	15.01	7.20	−11.6	−88	−5.5	−13.2
Guapán	E32	20/2/09	46.9	6.79	16500	62.1	2670	−78 84681	−2 70961	1.704	158.34	3.19	5.71	4.51	0.000	136.15	0.000	1.32	41.40	−4.7	−59	−5.3	−9.5
El Riñón	E33	20/1/00	74.5	6.83	4130	−173.9	2704	−79 06177	−2 92243	0.357	28.20	1.39	1.98	9.78	0.052	23.72	0.032	4.79	10.50	−11.4	−80	−4.9	−7.0
Portovelo	E34	21/2/09	52.4	7.94	2930	−307	661	−79 59724	−3 70292	0.305	19.07	0.35	0.01	7.63	0.125	22.27	0.026	5.19	0.45	−6.5	−38	−3.5	−8.2

Table 1 (Continued).

| Name	Sample	Date	T(°C)	pH	Cond. (uS cm^{-1})	Eh (mV)	Elevation (masl)	Longitude	Latitude	Li	Na	K	Mg	Ca	F	Cl	Br	SO$_4$	HCO$_3$	δ^{18}O	δD	δ^{13}C$_{TDIC}$	δ^{13}C$_{CO_2}$ computed
Rio amarillo	E35	21/2/09	19.4		51		661	−79 59724	−3 70292	0.001	0.16	0.02	0.11	0.24	0.001	0.05	0.000	0.08	0.50	−7.8	−46		
Jesús María	E36	21/2/09	42.6	9.18	499		187	−79 49335	−2 62662	0.004	3.76	0.03	0.00	0.49	0.012	0.64	0.000	3.16	0.65	−5.5	−30		
S.Vicente	E37	22/2/09	37.9	6.41	19700		70	−80 70098	−2 22794	0.004	103.57	0.39	0.02	137.94	0.000	236.05	1.499	0.00	9.50	0.6	−13		
Salinas de Bolivar	E38	23/2/09	17.0	6.84	68200		3519	−79 01984	−1 40779	10.808	723.83	61.83	25.29	65.91	0.000	840.25	1.069	41.45	32.85	4.7	−21		
Salinas de Bolivar Virgen	E39	23/2/09	14.8	6.39	11880		3530	−79 01984	−1 40779	1.454	95.61	8.67	3.55	24.53	0.000	106.89	0.100	5.91	17.80				
Salinas de Bolivar abajo	E40	23/2/09	19.4	7.55	5040		3511	−79 01984	−1 40779	0.597	39.66	3.68	1.24	1.33	0.000	44.97	0.034	2.30	1.90				
Rio Salinas	E41	23/2/09	10.7		177		3513	−79 01638	−1 40667	0.001	0.50	0.12	0.74	0.61	0.014	0.13	0.000	0.16	1.75				
Aguas Hediondas	E42	26/2/09	52.5	4.60	1850		3601	−77 90592	0 80966	0.040	8.75	1.03	3.95	4.54	0.230	3.49	0.003	16.99		−11.7	−87		
Chachimbiro	E43	26/2/09	51.2	6.90	5650		2531	−78 23185	0 45922	0.560	42.19	3.01	3.64	4.32	0.000	45.45	0.023	0.69	4.10	−8.4	−72	−1.0	−4.5
Pitzantzi	E44	26/2/09	31.8	7.04	4480		2696	−78 26421	0 42773	0.294	26.55	1.51	11.07	12.28	0.000	24.09	0.000	0.22	26.50	−9.4	−72	−0.4	
Cuicocha	E45	27/2/09	16.3	8.04	777		3070	−78 35771	0 29250	0.018	3.08	0.15	3.14	2.57	0.023	3.93	0.000	6.66	7.00				
El Salitre	E46	28/2/09	14.5	6.90	1550		3786	−78 40754	−0 60264	0.018	6.08	0.29	7.11	3.95	0.011	0.04	0.000	0.09	1.60	−12.7	−90	−9.3	−13.3
Rio Pita	E47	28/2/09	11.8	8.22	152		3787	−78 40754	−0 60264	0.001	0.47	0.08	0.45	0.54	0.051	1.51	0.000	2.88	4.00	−12.2	−87	−9.2	
Hummocks	E48	28/2/09	10.7	6.30	789		3792	−78 40826	−0 60357	0.016	2.77	0.14	3.32	2.22	0.007	2.14	0.000	0.42	6.10	−13.0	−93	−8.4	−13.2
Quilotoa	E49	14/4/09	22.0	6.76	12740	29.5	3510	−78 90967	−0 86242		100.34	4.87	59.83	18.27		117.38	0.12	50.21	12.45	−2.8	−39	−8.2	
Aguas caliente	E50	20/8/09	21.4	6.49	2700	7.6	2441	−78 67085	−0 43722		14.22	0.31	10.64	6.87	0.010	6.90	0.00	0.27	24.83	−10.2	−69	2.9	−1.3
Rio Quitasol	E51	20/8/09	10.5	8.10	177	132	2441	−78 67085	−0 43722		0.50	0.07	0.54	0.66	0.005	0.12	0.00	0.05	1.56	−10.6	−69	−10.9	
El Mozo	E52	4/12/09	14.9	5.82	231	−182	2810	−79 07551	−3 43819		1.05	0.11	0.19	0.68	0.008	0.95	0.00	1.41	0.60	−9.2	−56		
El Mozo	E53	4/12/09	13.0	5.11	36.4	243.2	2816	−79 07539	−3 43818		0.13	0.00	0.02	0.06	0.001	0.15		0.11	0.05	−7.7	−51		
El Mozo	E54	4/12/09	12.6	6.51	17.8	112.5	2762	−79 07997	−3 43439		0.05	0.02	0.02	0.05		0.03		0.04	0.08	−8.4	−50		
El Mozo	E55	4/12/09	11.9	4.88	30.5	335	2900	−79 07228	−3 43630		0.08	0.01	0.01	0.05		0.07	0.00	0.11	0.02	−9.0	−52		
El Mozo	E56	4/12/09	14.4	6.13	1330	−215	2761	−79 08023	−3 43448		7.02	0.27	1.45	5.83	0.022	14.72	0.01	7.95	6.00	−9.1	−57		
Puyango	E57	5/12/09	19.4		478	−352	800	−79 99094	−3 95697		4.34	0.01	0.00	0.04	0.094	0.44	0.00	0.72	3.60	−4.8	−24		
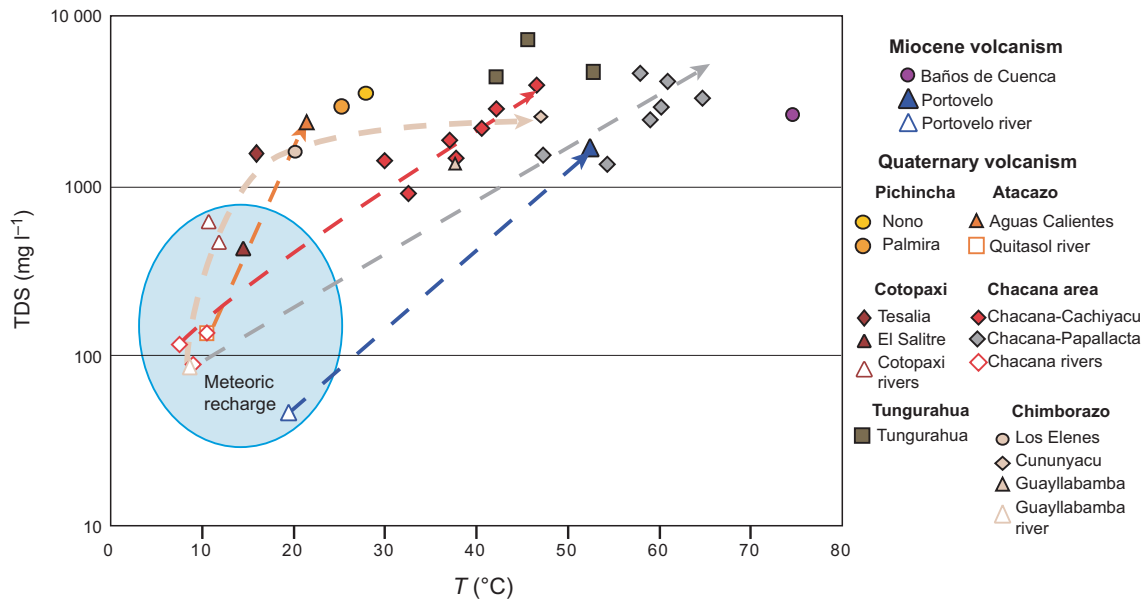
Fig. 3. Total dissolved salinity versus temperature. The meteoric recharge waters field is characterized by both low salinity and low temperature. The geothermal waters are characterized by high temperatures up to 74.5°C and salinity ranging between 1000 and 10000 mg l^{-1}.

relationship between the elevation of the springs and the altitude of the feeding or recharge areas. Nevertheless, Cununyacu (Chimborazo volcano), La Virgen, Santa Ana and El Salado (Tungurahua volcano), El Tingo, El Pisque, Ilaló and La Merced (Chacana Caldera), Guapante and Los Elenes waters plot in correspondence to an altitude about ≈1000 m higher than their elevation. For the former samples, this suggests that the summit areas of Chimborazo, Tungurahua and Chacana volcanoes, whose altitudes are 6310, 5020 and 4000 m, respectively, are the recharge areas of these springs. For Guapante and Los Elenes, the location of the recharge areas is less clear. On the other side, the few samples (i.e. San Vicente, Salinas, Guapán, Quilotoa, El Mozo and Puyango) plotting to the right of the theoretical vertical isotope gradient are likely affected by sub-aerial evaporation.

Major elements
Major ions (Li$^+$, Na$^+$, K$^+$, Mg^{2+}, Ca^{2+}, F$^-$, Cl$^-$, Br$^-$, NO$_3^{2-}$, SO$_4^{2-}$, HCO$_3^-$), SiO$_2$ and NH$_4^+$, were determined in the water samples and the analytical data are reported in Table 1.

As shown in the Langelier–Ludwig diagram (Fig. 5), sampled waters pertain to four different compositional families.
(1) Bicarbonate alkaline-earth waters. These waters are mainly the river samples, characterized by a very low TDS values (100–200 mg l^{-1}). They mostly represent the meteoric recharge of the investigated geothermal systems. Some waters (Nono, Pululahua, La Merced (Chacana), Tesalia, El Salitre, Hummocks and

Guapante,) with temperatures ranging 10.7–32.5°C also belong to this family, but their salinity is a little bit higher (400–3500 mg l^{-1})
(2) Bicarbonate-alkaline-waters (Chacana [Ilaló, Oyacachi, Lisco, Guachalá], Pitzantzi, Guayllabamba and Palmira) are characterized by a medium to high salinity (up to 4000 mg l^{-1}) and by high total dissolved carbon, probably because of dissolution of CO$_2$ (peripheral waters).
(3) Chlorine-sulphate-alkaline waters including most of the samples of Chacana caldera are characterized by high salinity (up to 5000 mg l^{-1}) and Salinas samples whose salinity is around 55 000 mg l^{-1}.
(4) Chlorine-sulphate-alkaline-earth waters characterized by medium (Tungurahua samples [La Virgen, El Salado, Santa Ana], Los Elenes and Cuicocha) to high (up to 14 000 mg l^{-1}; San Vicente) TDS values.

Interestingly, no water geochemical characteristic differentiates the thermal waters related to the Volcanic Front volcanoes (Chiles, Chachimbiro, Cuicocha, Pululahua, Pichincha, Atacazo, Quilotoa, Chimborazo) or to the Main Arc volcanoes (Chacana, Cotopaxi, Tungurahua), despite their different basement terranes.

Dissolved and bubbling gases

Several thermal waters are associated with gas phases showing strong bubbling gases that are CO$_2$-rich and characterized by a relatively high content of helium (up to 67 p.p.m vol; Guachalá water located in Chacana area).

The chemical composition of both dissolved and bubbling gases (Tables 2 and 3) plotted on the ternary
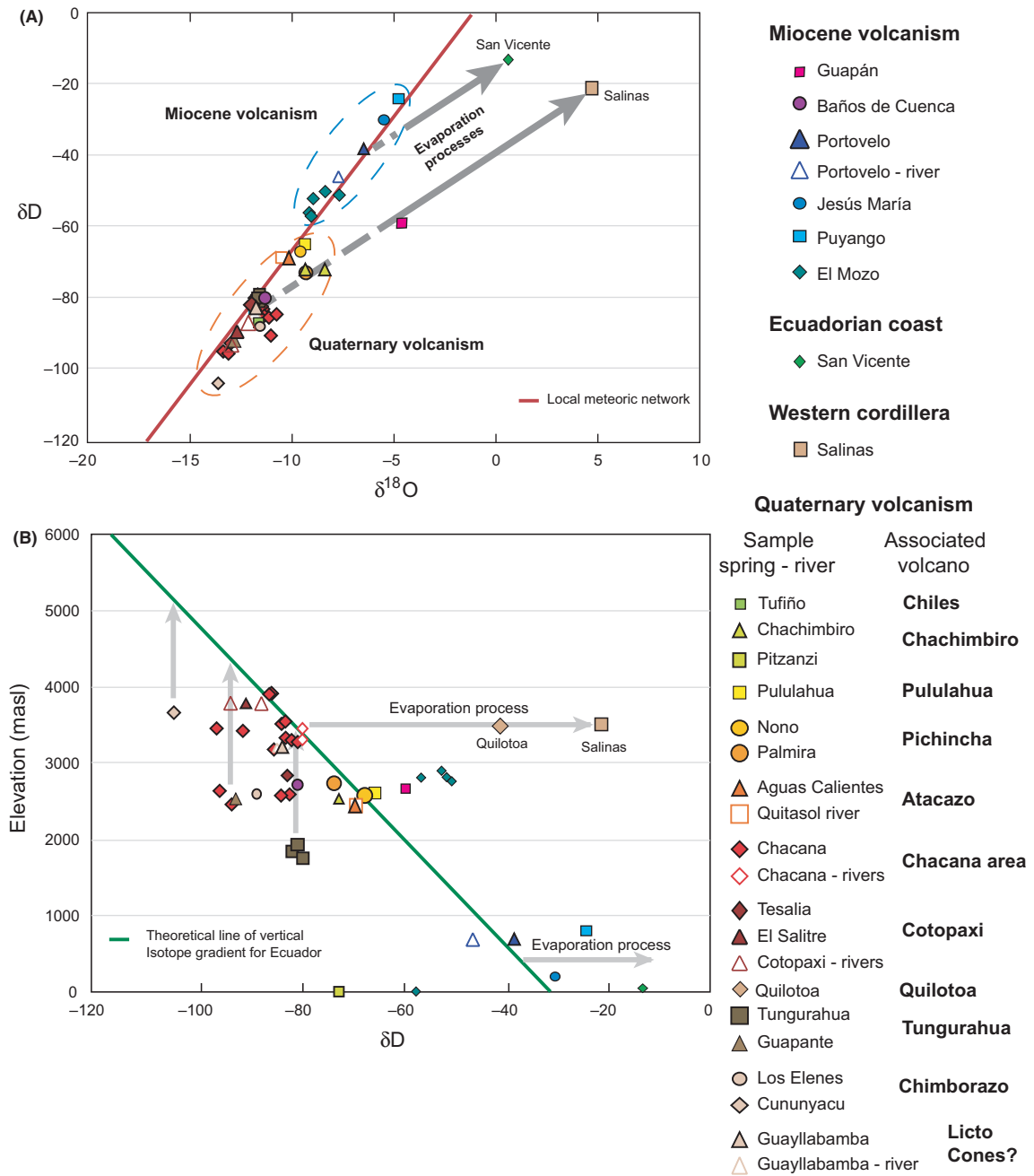
Fig. 4. (A) δD versus δ^{18}O. The isotopic compositions of sampled springs highlight a meteoric origin for all the samples. Local meteoric water-lines have been reported with these data. (B) Elevation of each sampling site versus δD isotopic composition; the theoretical line of vertical isotope gradient for Ecuador was added.

diagram CO_2-O_2-N_2 shows that all the samples related to the Quaternary arc fall close to the CO_2-corner. For Chacana area, a mixing with an atmospheric end-member seems evident. These samples show an alignment with O_2/N_2 ratio lower than that of air saturated water (ASW) highlighting an excess of nonatmospheric nitrogen and/or a consumption of oxygen (Fig. 6). This seems more evident for samples from Portovelo and San Vicente that are located very close to the N_2 corner.

Carbon dioxide and helium concentrations dissolved in the thermal waters are significantly higher than those of waters in equilibrium with the atmosphere (up to three orders of magnitude respect to ASW), suggesting contribution of CO_2 and helium from volatile-rich fluids.

To better define the origin of these gases, the isotope composition of C and He both on dissolved and bubbling gases was analysed. The carbon isotopes of CO_2 and the δ^{13}C$_{TDIC}$ of total dissolved carbon species range
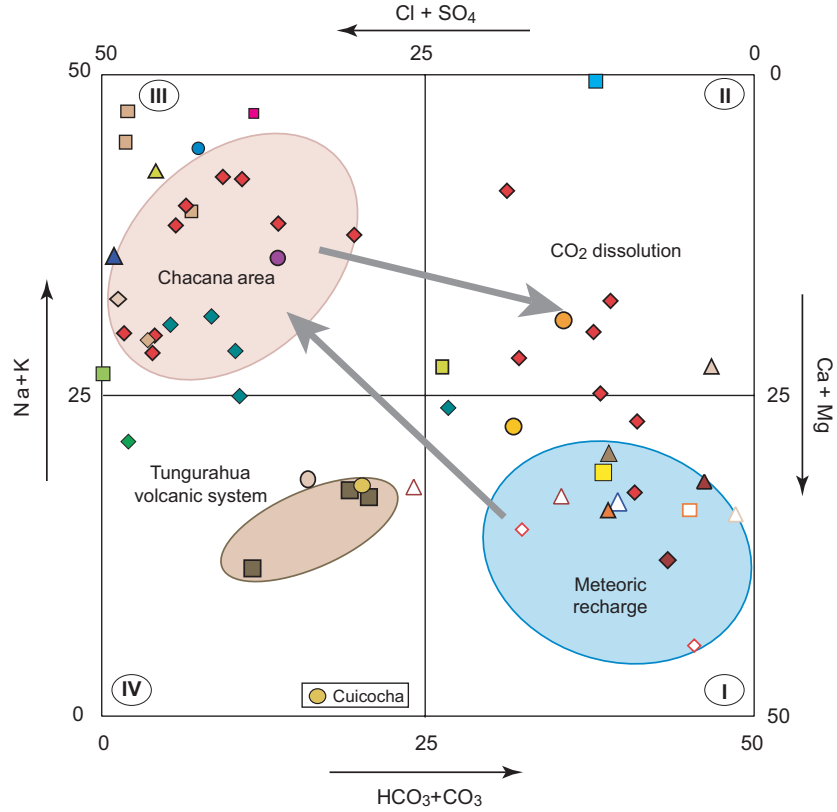
Fig. 5. Langelier–Ludwig diagram. Four families of samples have been identified on the basis of the chemical composition of thermal and cold waters. (i) Bicarbonate earth-alkaline waters characterized by low salinity and representative of meteoric recharge systems; (ii) Cl-SO$_4$ alkaline waters characterized by high salinity and representative of geothermal systems areas; (iii) bicarbonate alkaline waters characterized by high total dissolved carbon species and representative of peripheral waters; (iv) Cl-SO$_4$ earth-alkaline waters characterized by medium salinity and representative of Tungurahua area samples and by SanVicente thermal water characterized by high salinity around 19 000 mg l^{-1}. Symbols as on Fig. 4, except for Cuicocha which is located at the base of the diagram.

between −1.75 and −10.5 ‰ PDB (Table 3), suggesting a deep origin for these fluids, while few samples show very negative values around −30 ‰ PDB (Table 1) suggesting an organic origin and/or strong fractionation processes.

The helium isotope composition ranges between 0.1 and 7 R/R_a (R_a = 1.39*10^{-6}). The R/R_a values versus He/Ne ratio were plotted in Fig. 7 together with the values of mid-ocean ridge basalts (MORB), crust and air added for reference. A distribution in two different groups can be observed: the first one has values >2 R/R_a suggesting a variable contribution of mantle He (ranging from 24 to 89%); the second one has values R/R_a <1 indicating that the crustal component is, in some cases, largely predominant (ranging from 33 to 96%). Tungurahua, Guayllabamba, Pululahua, Tesalia, Cuicocha, Aguas Calientes and several fluid samples from the Chacana Caldera come from the first group. It is worth noting that such fluids discharge is related to Quaternary active volcanic systems. In contrast, Jesús María, Portovelo and San Vicente fluid discharges (all located south of 2°S) come from the second group. Jesús María is located at the boundary between the Western Cordillera foothills and the Coastal plain, and Portovelo and El Mozo are related to an old hydrothermal mineralizing system; San Vicente, given its proximity to the trench, might plausibly be related to fluids expelled from subducted sediments.

DISCUSSION

The isotopic composition of waters reveals a clear meteoric origin for all the sampled cold and thermal springs (Fig. 4A). The chemical composition is the result of water–rock interaction that occurs at different extents, as shown by the wide range of TDS values (Fig. 3).

The isotopic composition of TDIC is the result of the following chemical and isotope mass balance, where M stands for molarity, and the activity of CO$_3$ is considered negligible at pH <8.3:

$$\delta^{13}C_{TDIC} = (\delta^{13}C_{CO_2aq} * M_{CO_2aq} + \delta^{13}C_{HCO_3} * M_{HCO_3}) / M_{TDIC} \tag{1}$$

$$M_{TDIC} = M_{CO_2aq} + M_{HCO_3} \tag{2}$$

By using the enrichment factors ε_a and ε_b, (Mook et al., 1974; Deines et al., 1974)

$$\varepsilon_a = \delta^{13}C_{HCO_3} - \delta^{13}C_{CO_2g} = 9552/T_K - 24.1 \tag{3}$$

$$\varepsilon_b = \delta^{13}C_{CO_2aq} - \delta^{13}C_{CO_2g} = -0.91 + 0.0063 * 10^6/T_K^2 \tag{4}$$

Equation 1 can be written as follows:

$$\delta^{13}C_{CO_2g} = \delta^{13}C_{TDIC} - (\varepsilon_b * M_{CO_2aq}/M_{TDIC} + \varepsilon_a * M_{HCO_3}/M_{TDIC}) \tag{5}$$

Table 2 Chemical composition of dissolved gases. Values are expressed in cc per litre STP.

Sigla	He	H_2	O_2	N_2	CO	CH_4	CO_2
E1	1.92E-03	3.83E-02	5.30	23.14		8.38E-02	6.33
E2	1.98E-03	7.48E-04	2.27	16.53	2.44E-05	1.61E-03	12.82
E3	8.76E-04	0.00E+00	4.10	18.19	7.62E-05	3.04E-03	3.10
E4	5.28E-04	2.53E-02	1.40	4.90	4.56E-04	1.82E-02	125.21
E5			5.85	13.16		9.31E-05	1.04
E7	5.95E-04	1.10E-03	0.02	3.32	1.43E-04	4.84E-03	194.17
E8			0.04	7.80	3.67E-05	3.05E-03	285.22
E9	5.59E-04		0.05	6.41	1.48E-05	9.65E-03	83.01
E10	1.91E-03	5.11E-04	0.05	13.69		2.70E-03	92.65
E11	1.93E-03		1.69	22.98	1.36E-04	6.08E-03	174.45
E12		1.70E-03	0.62	21.95	2.75E-05	2.45E-02	95.59
E13	3.11E-04		3.19	14.66		5.17E-04	119.95
E14		2.93E-03	1.87	13.52		7.06E-03	256.91
E19	3.34E-04		0.02	6.34	2.75E-05	1.85E-02	359.97
E20	1.44E-04	2.59E-03	0.11	6.96		3.13E-03	222.10
E21	2.36E-04	0.00E+00	0.07	2.96		3.31E-01	564.61
E22	1.74E-04	0.00E+00	0.02	3.34		6.74E-02	582.19
E23	1.81E-04	0.00E+00	0.15	8.75		2.50E-04	476.45
E26	2.17E-04	5.90E-03	0.06	5.88		3.12E-04	226.05
E27		1.42E-02	0.64	5.78		1.77E-04	336.40
E28	3.31E-04	1.38E-03	0.02	10.33		2.80E-02	0.56
E29		2.45E-02	0.04	4.61		6.91E-02	283.27
E31	1.25E-04	2.70E-03	0.45	13.37		8.62E-04	14.95
E32	1.48E-04	2.70E-01	0.04	4.56		4.85E-03	272.10
E33	1.88E-04	3.06E-01	0.77	5.12		1.07E-02	104.26
E34	3.81E-04	1.36E-01	0.04	10.38		1.80E-02	0.89
E36	5.43E-04	5.18E-03	0.02	16.57		2.10E-02	0.67
E37		3.75E-02	0.06	8.69		9.52E-04	1.24
E43	1.90E-04	7.96E-01	0.06	6.48		2.66E-03	37.92
E46		0.00E+00	0.07	7.18		2.52E-02	39.00
E48	1.40E-04	0.00E+00	3.73	10.68		1.30E-04	113.96
E50		2.49E-03	0.06	3.71		1.56E-03	455.40

Next, the isotope composition of CO_2 gas in equilibrium with the aquifers considering the dissolved CO_2 and HCO_3 amounts at the temperature of aquifer using the eq. 5 was calculated (Inguaggiato *et al.* 2000, 2005). The obtained values are reported in Table 1.

Figure 8 shows the computed isotopic composition of CO_2 gas and the $\delta^{13}C_{CO_2}$ of bubbling gases both versus the total C (HCO_3 + CO_2diss). The plotted data show a wide variability for the amount of total carbon covering three orders of magnitude (from <1 meq l^{-1} to more than 100 meq l^{-1}). This wide variability reflects the progress of gas–water interaction processes and could be because of adding/removal CO_2 processes in the aquifers (Inguaggiato *et al.* 2000, 2005). Conversely, the carbon isotope composition shows a narrow variability around a magmatic signature (−5 to −8‰) suggesting a common deep magmatic origin for the CO_2 interacting with the thermal waters even if they display different degrees of gas–water interaction.

Only three thermal water samples from the Papallacta area and one of the Papallacta river show very negative values (around −30‰) with a lower amount of total dissolved

carbon between 1 and 4 meq l^{-1}. These negative values suggest an organic matter origin for the carbon and/or kinetic fractionation processes because of carbon removal in response to carbonate precipitation. In fact, in these thermal waters, lower concentrations of dissolved carbon were measured and the presence of travertine deposits is evident in this area.

The isotope composition of He in the bubbling gases was analysed to constrain the origin of this gas. The carbon isotope composition versus R/R_a corrected (where R_a is equal to $1.39*10^{-6}$) is plotted in Fig. 9. The distribution of data confirms a mantle-like signature for these fluids; in fact, the carbon isotope ratios of bubbling-CO_2 range between −5 and −10‰, and almost all of the bubbling samples have He isotope composition ranging between 2 and 7 R/R_a.

The isotope composition of He versus the latitude of samples has been plotted in Fig. 10 to investigate a possible relationship between the origin of fluids and their location on the Ecuadorian Arc. MORB, crust and air are plotted as references. All the samples located to the north of 2°S, in the active Quaternary volcanic arc, display He isotope ratios from 2 to 7 R/R_a, while the samples below

Table 3 Chemical composition of bubbling gases. The values of O_2, N_2 and CO_2 are expressed in % vol, while the values of H_2, CO and CH_4 are expressed in p.p.m vol. The isotopic composition of CO_2 gas is expressed in ‰ PDB standard.

Sample	H_2 p.p.mVol	O_2 %Vol	N_2 % Vol	CO p.p.mVol	CH_4 p.p.mVol	CO_2 %Vol	R/R_a	He/Ne	[He] corr	[Ne] corr	R/R_a c	$\delta^{13}C(CO_2)$
E4		0.89	15.82	1.30	1446	84.04	7.09	59.36	136.52	2.30	7.12	−6.79
E8		0.12	37.66	0.50	126	61.88	4.08	11.80	67.84	5.75	4.16	−10.5
E9		0.54	0.55	1.30	103	98.40		0.67	0.50	0.75		−5.41
E14							6.01	3.44	0.00	0.00	6.46	
E15		4.21	16.83	4.00	3	77.89	3.91	4.28	0.54	0.13	4.15	−5.13
E17		14.82	59.46	1.10	18	25.83	2.27	1.51	0.61	0.40	2.60	−6.79
E20		0.08	0.22	0.30	2140	98.25	2.84	1.33	0.26	0.19	3.42	−5.03
E21			1.12		2	95.71	3.54	6.94	1.45	0.21	3.66	−3.84
E22		2.45	9.74	0.40	377	87.25		1.96	0.44	0.23		−2.93
E23		1.74	13.14	0.60	2	82.79	6.62	8.62	5.58	0.65	6.83	−7.79
E25		0.07	0.18	0.20	16	100.00	4.84	5.08	0.73	0.14	5.10	−7.8
E26		0.18	1.01	6.00	54	98.24		0.35	2.92	8.25		−6.84
E27		0.10	0.24		4	99.74	3.64	1.95	0.43	0.22	4.16	−7.11
E29		0.61	4.21	0.70	1	93.62	2.02	6.58	4.30	0.65	2.07	−10.19
E32	6	0.20	0.61	0.70	330	100.00	0.74	2.62	0.91	0.35	0.70	−9.94
E34		0.17	95.90	0.40	3225	0.16	0.94	97.61	542.37	5.56	0.93	
E36							0.45	1.63	0.00	0.00	0.34	
E37	7	0.10	0.85	0.30	981500	0.02	0.11	12.59	6.82	0.54	0.08	
E38	16	0.57	2.25	4.40	0	93.44		0.30	3.45	11.47		−1.75
E39		0.12	1.25	5.00	17	97.34						−2.47
E42	24	0.03	2.84	21.00	12	93.24		0.33	3.97	12.09		−3.17
E43							0.43		0.00	0.00		
E45		4.23	59.26	4.20	873	37.43	5.73	3.18	8.47	2.66	6.26	−3.94
E49		0.42	3.08	79.00	8	96.33	1.87	1.72	0.15	0.09	2.07	−4.94
E50		0.19	1.13	5.30	16	97.61	3.03	2.04	0.25	0.12	3.41	−6.07
E52							0.67	0.51	5.82	11.49	0.11	
E54							0.76	0.49	3.88	7.94	0.33	

this latitude, where no active volcanism has been recognized because the Miocene, show a more crustal-like component with lower He-isotopes ratios (0.1–1 R/R_a).

To better clarify the origin of these gases and the processes that they underwent during their ascent towards the surface, the $C/^3He$ ratio has plotted against the isotopic composition of He, including the fields of MORB, hot spots, carbonate sediments and the continental crust (Fig. 11; Marty & Jambon 1987; Varekamp et al. 1992; Sano & Marty 1995; Hilton et al. 1993). The bubbling gases show a wide range for log $C/^3He$ between 6.5 and 12.5, and with R/R_a values between 0.1 and 7. The values displayed by carbon and helium in samples taken in Chacana area are consistent with deep mantle–related fluids. CO_2 addition processes can be invoked for Tungurahua volcanoes fluids (E25–E27). A contamination of carbon addition related to continental crust and/or carbonate sediments is evident for the San Vicente area, which shows higher log $C/^3He$ and lower R/R_a values (12 and 0.1, respectively). Owing to the proximity of this spring to the trench, the addition of carbon by carbonate sediments is likely. The relatively low values of log $C/^3He$ (6.5) with R/R_a values of 0.9 for Portovelo indicate a more crustal-like source. This helium contains almost 90% of crustal helium and approximately 10% of MORB-type helium,

supporting both a removing carbon process and, more likely, a crust-like helium contribution for this sample. Moreover, in the CO_2-N_2-CH_4 ternary diagram (Fig. 12), three different groups of gases are clustered, corresponding to the Tungurahua, Portovelo and San Vicente systems, CO_2, N_2 and CH_4 dominated, respectively.

Finally, to corroborate the origin and the processes undergone by these fluids, the isotopic composition of nitrogen was measured on the Tungurahua and Portovelo samples, and the carbon isotope composition of CH_4 in San Vicente sample. The main potential sources of nitrogen in volcanic and hydrothermal fluids are (i) the atmosphere; (ii) the upper mantle, including both unaltered subducting oceanic crust and mantle wedge; (iii) the lower mantle; and (iv) the sediments, including subducted oceanic sediments and the continental crust. Each of these reservoirs has distinct $\delta^{15}N$ values. Atmospheric nitrogen has been conventionally used as an international reference ($\delta^{15}N = 0$‰). The upper mantle, investigated through analyses on MORB and diamonds, revealed the presence of a light nitrogen component with typical $\delta^{15}N$ values in the range -3‰ to -8‰ (Cartigny 1997; Marty and Hubert, 1997). Recently, anomalously negative $\delta^{15}N$ values of -15‰ have been inferred for the lower mantle beneath the Indonesian plate (Mohapatra & Murty 2004; Clor et al.
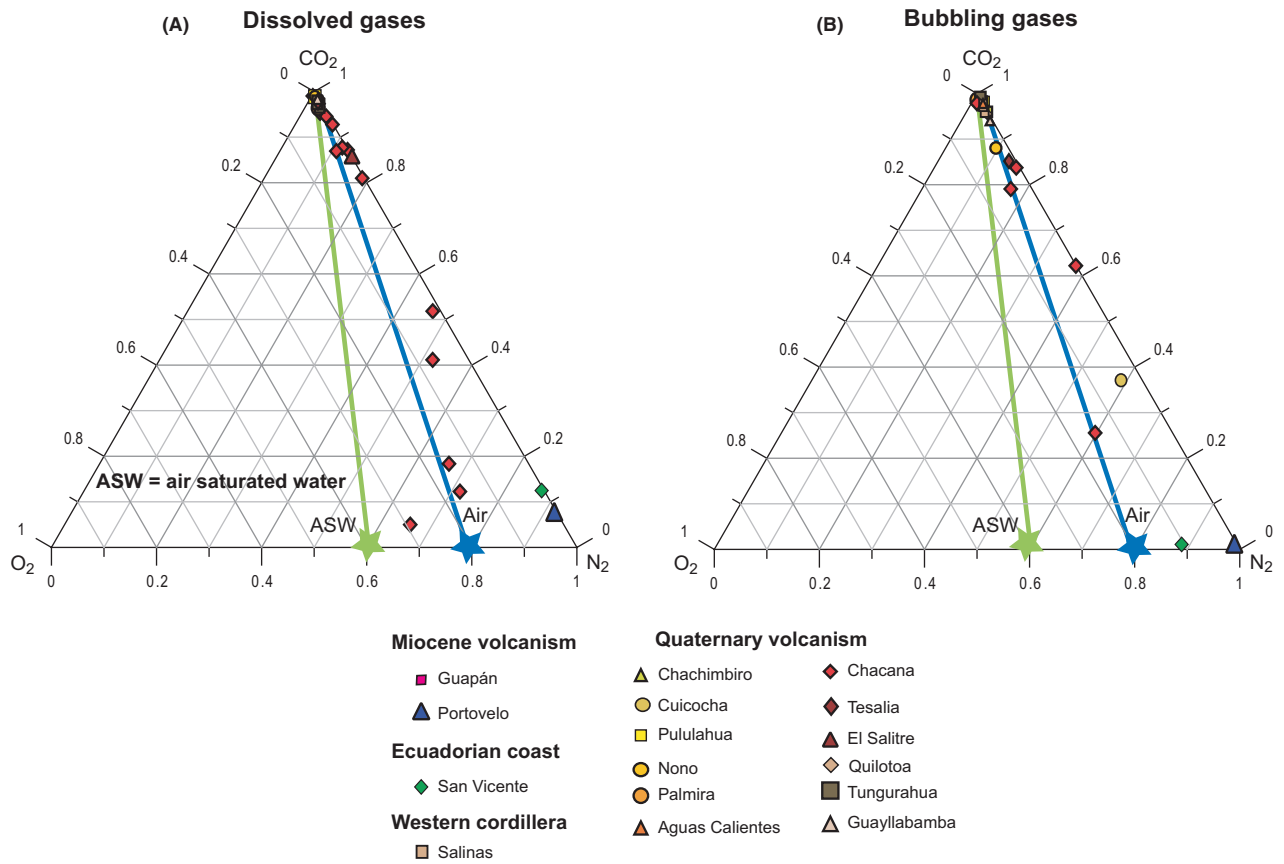
Fig. 6. (A) CO_2-N_2-O_2 diagram for dissolved gases and (B) for bubbling gases. All the samples show a mixing of CO_2 and Nitrogen with N_2/O_2 ratio higher than the air saturated water ratio plotted as reference.
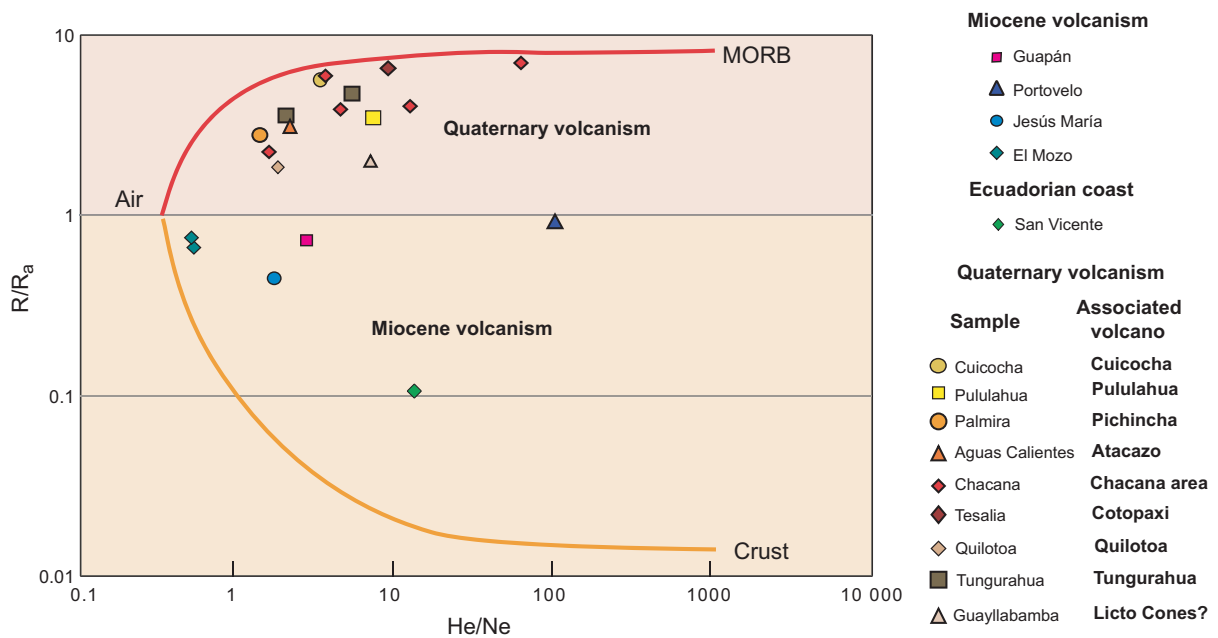
Fig. 7. R/R_a values versus He/Ne ratio diagram of sampled bubbling gases. Air, mid-ocean ridge basalts and crust fields are reported as reference. The samples display a distribution in two main groups above 2 R/R_a and below 1 R/R_a. The He/Ne ratios range between about 1 and 100.
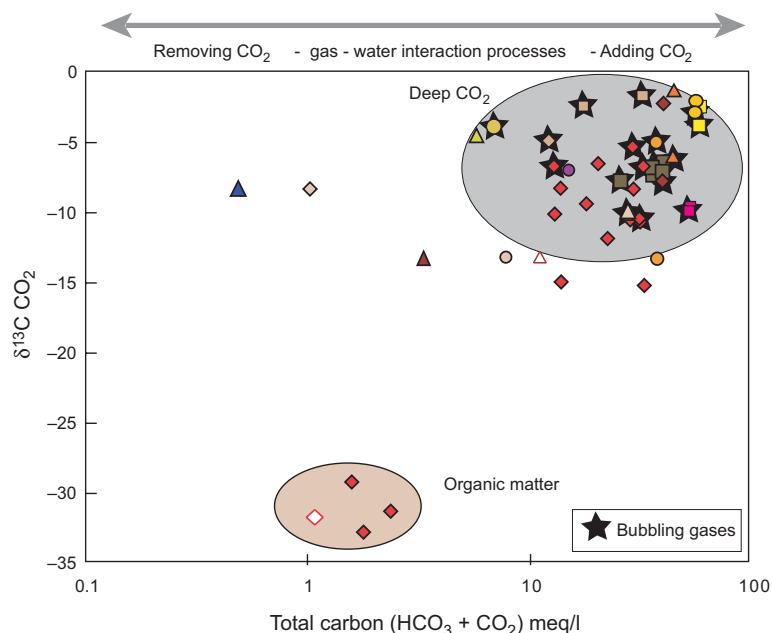
Fig. 8. $\delta^{13}C$ of computed CO_2 gas from carbon isotope composition of TDIC and the $\delta^{13}rmC_{CO_2}$ of bubbling gases both versus total amount of dissolved carbon species (HCO_3 + dissolved CO_2). The wide variability showed for the total carbon amount reflects probably adding/removing CO_2 processes in the aquifers. The carbon isotope composition shows a narrow variability (-5 to $-8‰$) indicating a common origin for the dissolved carbon in thermal waters. The very negative values (around $-30‰$), with lower amount of total dissolved carbon, could indicate a different origin (organic) or be related to kinetic fractionation processes.

2005) and for the Nicaraguan volcanic front (Elkins *et al.* 2006). Moreover, Inguaggiato *et al.* (2009) have recently reported extremely low $\delta^{15}N$ values of -16 and -15 ‰ for the excess N_2 in the volcanic gas samples, respectively, from Cabo Verde islands and Iceland. In contrast, typical $\delta^{15}N$ values for a sedimentary component are generally enriched compared to those of the atmosphere ($\delta^{15}N$ = $+7‰$, Sadofsky and Bebout, 2004; Sano *et al.* 2001; Mingran and Brauer, 2001).

Nitrogen isotope compositions were measured on only two samples, Portovelo and Tungurahua which, respectively, represent the nitrogen- and CO_2-dominant samples. The nitrogen data have been corrected for atmospheric contamination on the basis of the following equations (Inguaggiato *et al.* 2004b, 2006):

$$\delta^{15}N_{corr} = (\delta^{15}Nmeas/N_{2_{excess}}(\%)) * 100 \quad (6)$$

$$N_{2_{excess}}(\%) = \frac{N_{2_{observed}} - N_{2_{atmospheric}}}{N_{2_{observed}}} * 100 \quad (7)$$

$$N_{2_{atmospheric}} = {}^{36}Ar_{observed} * \left(\frac{N_2}{{}^{36}Ar}\right)_{ASW} \quad (8)$$

The $\delta^{15}N$ values corrected for air contamination have been plotted versus R/R_a in Fig. 13, together with the field of upper mantle and crust as references. The distribution of samples highlights a different origin for both systems, $\delta^{15}N$ = $-5‰$, 5 R/R_a and $\delta^{15}N$ = $+5‰$, 0.9 R/R_a, respectively, for Tungurahua and Portovelo. These values are compatible with the geodynamic setting of the Ecuadorian volcanoes, in fact Tungurahua volcano fluids, characterized by significant He-mantle signature (around 60%), is located in the recent active volcanism area (above 2°S) and has been active since 1999, while the fluid manifestation of Portovelo, characterized by a prevalent He-sedimentary-crustal signature (around 90%), is located in the ancient Miocene volcanic area (below 2°S).

Finally, the isotope composition of carbon of CH_4 in the San Vicente sample, characterized by methane-rich fluids (98.1% Vol), shows a value of -39 ‰ versus
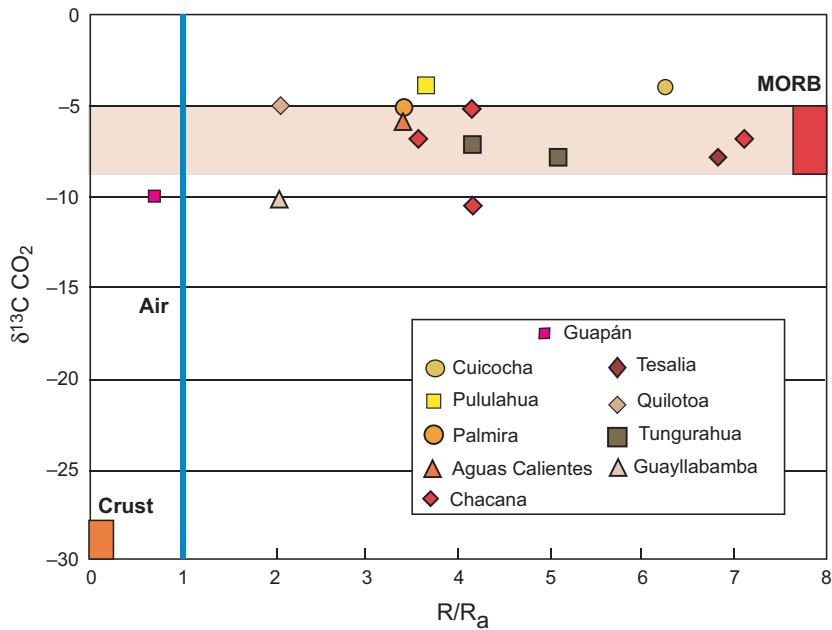
Fig. 9. $\delta^{13}C_{CO_2}$ of bubbling gas versus R/R_a; mid-ocean ridge basalts and crust values are plotted as reference. The carbon isotope displays a very narrow range confirming the common origin of carbon for these fluids. The R/R_a values from 2 up to 7 for the bubbling free gases are indicative of a magmatic origin for the majority of samples.
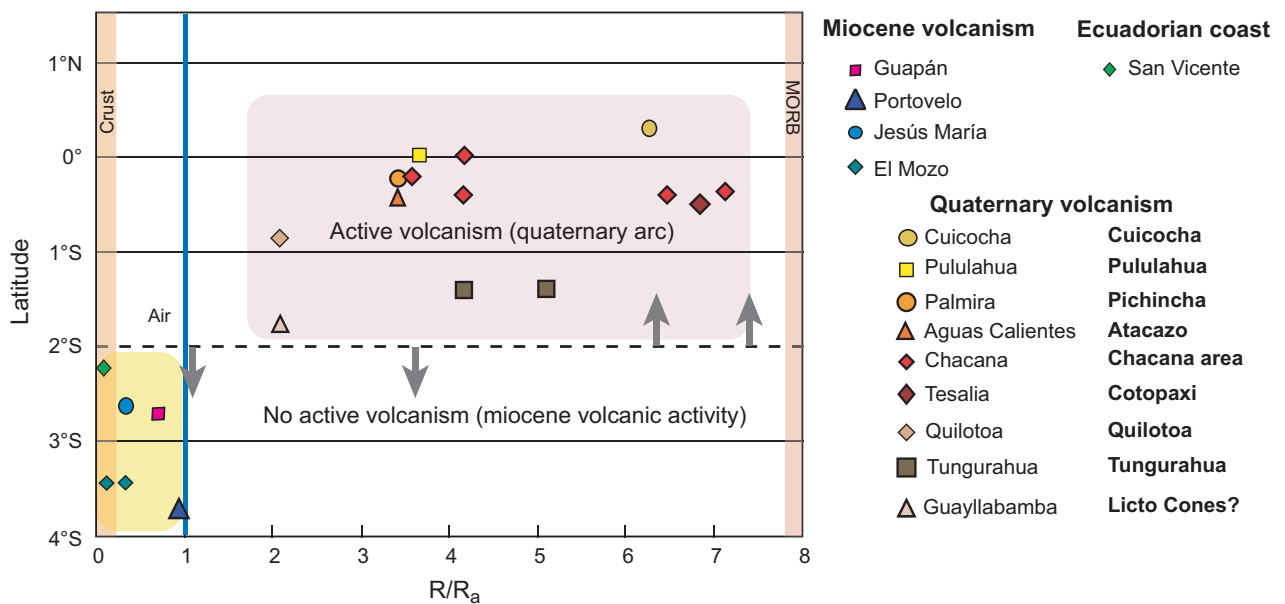
Fig. 10. Helium isotopic composition versus the Latitude of sampling sites. A clear geographic distribution of samples in two geochemical groups is evident. All the samples located to the north of 2°S highlight the origin of these fluids from an active volcanic arc (R/R_a from 2 to 7), while all the samples located below 2°S reflect an origin from a nonactive volcanic arc (R/R_a below 1).

PDB. This value suggests a thermogenic origin for these fluids.

CONCLUSIONS

The first characterization of hydrothermal fluids related to volcanic systems of the Volcanic Ecuadorian chains highlights the key role of volatiles.

The geochemical composition of the sampled thermal waters is the result of strong water–rock interaction processes that drive the dissolution of minerals on the basis of the physico-chemical conditions of aquifers (pH, T, P, redox conditions) and show, on the basis of deuterium and oxygen isotopes composition, a clear meteoric origin.

Interestingly, no clear water geochemical differences can be discerned between the hydrothermal systems linked to
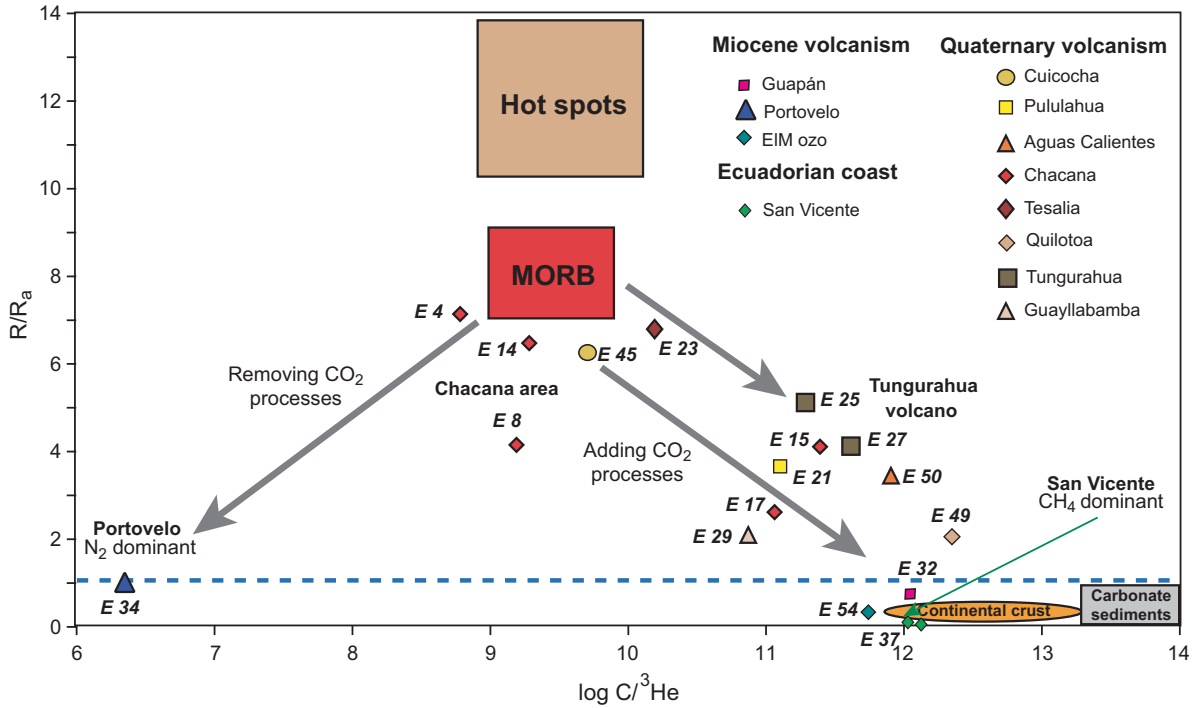
Fig. 11. Log $C/^3He$ versus R/R_a of bubbling gases. The distribution of plotted samples reflects two different kinds of processes: gas–water interaction processes with fluids with magmatic origin and carbon adding/removing processes. The fluids of Chacana area show higher helium isotope values with Log $C/^3He$ around 10. San Vicente area shows lower R/R_a values (up to 0.1) with higher Log $C/^3He$ up to 12, highlighting CO_2 adding processes. Conversely, Portovelo sample area shows values of R/R_a around 1 with a very low value of Log $C/^3He$ (around 6) indicating strong CO_2 removing processes.
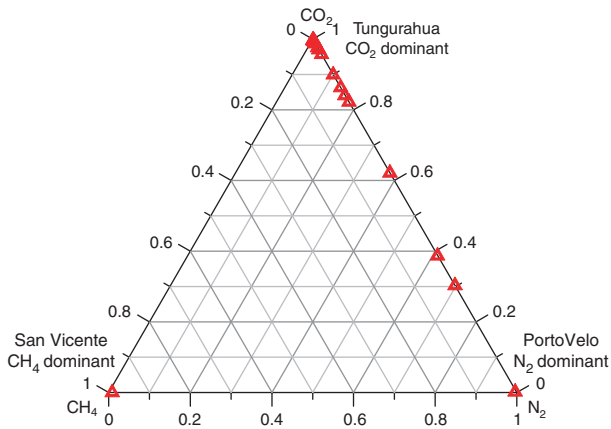
Fig. 12. The chemical composition of bubbling gases samples plotted on the CO_2-N_2-CH_4 diagram highlights the presence of three groups of samples: Tungurahua, Portovelo and San Vicente areas, respectively, CO_2, N_2 and CH_4 dominant samples. A mixing between CO_2 and N_2 dominant samples is evident, too.
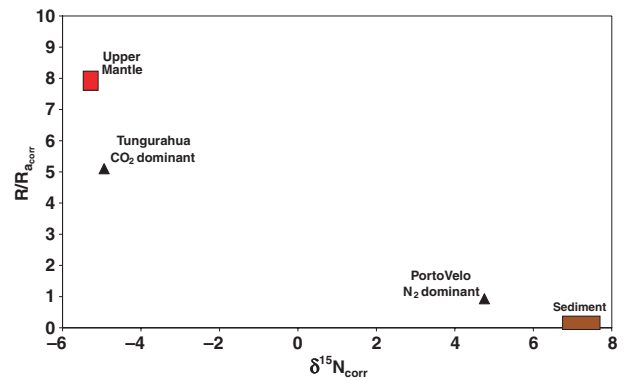

Fig. 13. Nitrogen and helium isotope compositions, both corrected for air contamination, of Tungurahua and Portovelo samples have been plotted. Two clear different origins (magmatic and sedimentary) are evident, respectively, for the Tungurahua and Portovelo samples.

the Volcanic Front volcanoes or the Main Arc ones, despite their different basements.

These fluids highlight a MORB-like isotopic signature of CO_2 at $R/R_a > 2$. The helium isotope composition ranges from 0.1 to 7.1 R/R_a. This allowed the division of the samples in two distinct groups, above 2 and below 1 R/R_a,

respectively. These two groups of samples correspond to the geographical limit of the active volcanic arc in Ecuador. The springs group with higher R/R_a values lies to the north of 2°S (active volcanism), and the springs group with lower values lies to the south of 2°S (extinct volcanism).

The nitrogen isotope compositions of discharged fluids corroborate the different origin of these two groups of fluids (−5 and +5 $\delta^{15}N$, respectively for Tungurahua and Portovelo samples) with a clear geographic distribution, which

highlights the powerful tool of the isotopes to discriminate different sources.

On the basis of this preliminary fluid characterization exercise and considering the strong gas–water interaction between deep magmatic fluids and thermal waters associated to volcanic systems, it is possible to identify sensible sites for starting a systematic geochemical monitoring activity and complementary research for geothermal energy exploration.

ACKNOWLEDGEMENTS

REFERENCES

Aspden JA, Litherland M (1992) The geology and Mesozoic collisional history of the Cordillera Real, Ecuador. *Tectonophysics*, **205**: 187–204.

Aspden JA, Fortey N, Litherland M, Viteri F, Harrison SM (1992a) Regional S-type granites in the Ecuadorian Andes: Possible remnants of the breakup of western Gondwana. *Journal of South American Earth Sciences*, **6**, 123–32.

Aspden JA, Harrison SH, Rundle CC (1992b) New chronological control for the tectono-magmatic evolution of the metamorphic basement, Cordillera Real and El Oro Province of Ecuador. *Journal of South American Earth Sciences*, **6**: 77–96.

Beate B, Salgado R (2005) *Country Geothermal update for Ecuador, 2000–2005.* Proceedings World Geothermal Congress, Antalya – Turkey.

Beate B, Monzier M, Spikings R, Cotten J, Silva J, Bourdon E, Eissen JP (2001) Mio-Pliocene adakite generation related to flat subduction in southern Ecuador: the Quimsacocha volcanic center. *Earth and Planetary Science Letters*, **192**, 561–70.

Capasso G, Inguaggiato S (1998) A simple method for the determination of dissolved gases in natural waters: an application to thermal waters from Vulcano island. *Applied Geochemistry*, **13**, 631–42.

Cartigny P, Boyd SR, Harris JW, Javoy M (1997) Diamonds and isotopic composition of mantle nitrogen. *Terra Nova*, **9**, 175–9.

Clor LE, Fischer TP, Hilton DR, Sharp ZD, Hartono U (2005) Volatile and N isotope chemistry of the Molucca Sea collision zone: tracing source components along the Sangihe Arc, Indonesia. *Geochemistry Geophysics Geosystem.* 6. doi:10.1029/2004GC000825.

Cosma L *et al.* (1998) Pétrographie et géochimie des unités magmatiques de la Cordillère Occidental d'Equateur (0°30′S): implications tectoniques. *Bulletin de la Société Géologique de France*, **169**, 739–51.

Deines P, Langmuir D, Herman RS (1974) Stable carbon isotope ratio and the existence of a gas phase in the evolution of carbonate groundwaters. *Geochimica et cosmochimica acta*, **38**, 1147–64.

Elkins LJ, Fischer TP, Hilton DR, Sharp ZD, McKnight S, Walker J (2006) Tracing nitrogen in volcanic and geothermal volatiles from the Nicaraguan volcanic front. *Geochimica et Cosmochimica Acta* , **70**, 5215–35.

Goosens PJ, Rose W (1973) Chemical composition and age determination of tholeiitic rocks in the Basic Igneous Complex, Ecuador. *Geological Society of America Bulletin*, **84**, 1043–52.

Gutscher MA, Malavieille J, Lallemand S, Collot JY (1999) Tectonic segmentation of the North Andean margin: impact of the Carnegie Ridge collision. *Earth and Planetary Science Letters*, **168**, 255–70.

Hall ML, Beate B (1991) *El Volcanismo Plio-cuaternario en los Andes del Ecuador.* Est. Geogr. Vol 4. Corp.Edit.Nacional. Quito.

Hein RJ, Yeh H-W (1983) Oxygen-isotope composition of secondary silica phaes, Costa Rica Rift, Deep Sea Drilling Project Leg 69. *Deep Sea Drilling Project Initial Reports*, **69**, 423–9.

Hilton DR, Hammerschmidt K, Teufel S, Friedrichsen H (1993) Helium isotope characteristics of Andean geothermal fluids and lavas Earth and Planetary. *Science Letters*, **120**, 265–82.

Hughes R, Pilatasig L (2002) Cretaceous and Tertiary terrane accretion in the Cordillera Occidental of the Andes of Ecuador. *Tectonophysics*, **345**, 29–48.

Inguaggiato S, Rizzo A (2004) Dissolved helium isotope ratios in ground-waters: a new technique based on gas-water re-equilibration and its application to Stromboli volcanic system. *Applied Geochemistry*, **19**, 665–73.

Inguaggiato S, Pecoraino G, D'Amore F (2000) Chemical and isotopical characterization of fluid manifestations of Ischia Island (Italy). *Journal of Volcanology and Geothermal Research*, **99**, 151–78.

Inguaggiato S, Taran YA, Grassa F, Capasso G, Favara R, Varley N, Faber E (2004b) Nitrogen isotopes in thermal fluids of a forearc region (Jalisco Block, Mexico): evidence for heavy nitrogen from continental crust. *Geochemistry Geophysics Geosystem*, **5**, Q12003.

Inguaggiato S, Martin-Del Pozzo AL, Aguayo A, Capasso G, Favara R (2005) Isotopic, chemical and dissolved gas constraints on spring water from Popocatepetl (Mexico): evidence of gas-water interaction magmatic component and shallow fluids. *Journal of Volcanology and Geothermal Research*, **141**, 91–108.

Inguaggiato S, Grassa F, Capasso G, Favara R, Rizzo A, Taran Y (2006) Simultaneous determination of ^{36}Ar and N_2 content together with $\delta^{15}N$ values in gas samples: examples from different arc-related volcanic systems AGU Fall Meeting 2006.V33A-0638.

Inguaggiato S, Taran Y, Fridriksson T, Melian G, D'Alessandro W (2009) Nitrogen isotopes in volcanic fluids of different geodynamic settings. *Geochimica et Cosmochimica Acta* , **73**(Suppl.), A569.

Kellogg JN, Vega V (1995) Tectonic development of Panama, Costa Rica, and the Columbian Andes: constraints from global positioning system geodetic studies and gravity. In: *Geologic and Tectonic Development of the Caribbean Plate Boundary in Southern Central America* (ed. Mann P), pp. 75–86. Geological Society of America Bulletin, Boulder, Colorado.

Lapierre H *et al.* (2000) Multiple plume events in the genesis of the peri-Caribbean Cretaceous oceanic plateau province. *Journal of Geophysical Research*, **105**, 8404–21.

Lavenu A *et al.* (1992) New K-Ar age dates of Neogene and Quaternary volcanic rocks from the Ecuadorian Andes : implications for the relationship between sedimentation, volcanism, and tectonics. *Journal of South American Earth Sciences*, **5**, 309–20.

Lebrat M, Megard F, Dupuy C, Dostal J (1987) Geochemistry and tectonic setting of pre-collision Cretaceous and Paleogene volcanic rocks of Ecuador. *Bulletin of the Geological Society of America*, **99**, 569–78.

Litherland M, Aspden JA, Jemielita RA (1994) The metamorphic belts of Ecuador, Overseas memoir 11. British Geological Survey.

Lonsdale P (1978) Ecuadorian subduction system. *The American Association of Petroleum Geologist Bulletin*, **62**, 2454–77.

Lonsdale P, Klitgord KD (1978) Structure and tectonic history of the eastern Panama Basin. *Geological Society of America Bulletin*, **89**, 981–99.

Luzieux LDA, Heller F, Spikings R, Vallejo C, Winkler W (2006) Origin and Cretaceous tectonic history of the coastal Ecuadorian forearc between 1[deg]N and 3[deg]S: paleomagnetic, radiometric and fossil evidence. *Earth and Planetary Science Letters*, **249**, 400–14.

Marty B, Jambon A (1987) $C/^3He$ in volatile fluxes from the solid earth: implications for carbon geodynamics. *Earth Planetary Science Letters*, **83**, 16–26.

Marty B, Humbert F (1997) Nitrogen and argon isotopes in oceanic basalts. *Earth Planetary Science Letters*, **152**, 101–12.

Michaud F *et al.* (2005) Fields of multi-kilometer scale sub-circular depressions in the Carnegie Ridge sedimentary blanket: effect of underwater carbonate dissolution? *Marine Geology*, **216**, 205–19.

Mingram B, Brauer K (2001) Ammonium concentration and nitrogen isotope composition in metasedimentary rocks from different tectonometamorphic units of the European Variskan Belt. *Geochimica et cosmochimica acta*, **65**, 275–87.

Mohapatra RK, Murty SVS (2004) Nitrogen isotopic composition of the MORB mantle: a reevaluation. *Geochemistry, Geophysics, Geosystems*, **5**, Q01001.

Mook WG, Bemmerson JC, Steverman WH (1974) Carbon isotope fractionation between dissolved bicarbonate and gaseous carbon dioxide. *Earth and Planetary Science Letters*, **22**, 169–76.

Pennington WD (1981) Subduction of the eastern Panama Basin and seismotectonics of northwestern South America. *Journal of Geophysical Research*, **86**, 10753–70.

Reynaud C, Jaillard E, Lapierre H, Mamberti M, Mascle G (1999) Oceanic plateau and island arcs of southwestern Ecuador:Their place in the geodynamic evolution of northwestern South America. *Tectonophysics*, **307**, 235–54.

Sadofsky SJ, Bebout GE (2004) Nitrogen geochemistry of subducting sediments: new results from the Izu-Bonin-Mariana margin and insights regarding global nitrogen subduction. *Geochemistry Geophysics Geosystems*, **5**, Q03115, doi: 10.1029/2003GC000543.

Sallares V, Charvis P (2003) Crustal thickness constraints on the geodynamic evolution of the Galapagos Volcanic Province. *Earth and Planetary Science Letters*, **214**, 545–59.

Sano Y, Takahata N, Nishio Y, Fischer TP, Williams SN (2001) Volcanic flux of nitrogen from the earth. *Chemical geology*, **171**, 263–71.

Sano Y, Marty B (1995) Origin of carbon in fumarolic gas from island arcs. *Chemical Geology* , **119**, 265–74.

Sano Y, Wakita H (1985) Geographical distribution of $^3He/^4He$ in Japan: implications for arc tectonics and incipient magmatism. *Journal of Geophysical Research* , **90**, 8729–41.

Trenkamp R, Kellogg JN, Freymueller JT, Mora HP (2002) Wide plate margin deformation, southern Central America and northwestern South America, CASA GPS observations. *Journal of South American Earth Sciences*, **15**, 157–71.

Varekamp JC, Kreulen R, Poorter RPE, Van Bergen MJ (1992) Carbon sources in arc volcanism, with implications for the carbon cycle. *Terra Nova*, **4**, 363–73.

Witt C *et al.* (2006) Development of the Gulf of Guayaquil (Ecuador) during the Quaternary as a response to the North Andean Block tectonic escape Tectonics **25**: TC3017, doi: 10.1029/2004TC001723.